THE ASTROPHYSICAL JOURNAL, 170:207–217, 1971 December 1

THE SMALL-SCALE STRUCTURE OF RADIO GALAXIES AND QUASI-STELLAR SOURCES AT 3.8 CENTIMETERS

M. H. COHEN, W. CANNON, G. H. PURCELL, AND D. B. SHAFFER
Owens Valley Radio Observatory,* California Institute of Technology

J. J. BRODERICK AND K. I. KELLERMANN†
National Radio Astronomy Observatory, Green Bank, West Virginia

AND

D. L. JAUNCEY‡
Cornell-Sydney University Astronomy Center, Cornell University
Received 1971 June 28; revised 1971 July 21

ABSTRACT

We have observed fringes from 31 compact radio sources, including eight known or suspected galaxies and 20 known or suspected QSSs, by using the Goldstack interferometer at $\lambda = 3.8$ cm ($d/\lambda = 10^8$). Fringe visibility curves were obtained for nine sources showing structure on a scale of 10^{-3} sec of arc, and simple models are fitted to the data. Results for 3C 273 and 3C 279 are compared with data taken by Knight *et al.* at an earlier epoch. The apparent changes in brightness distribution of 3C 273 and 3C 279 are difficult to explain.

I. INTRODUCTION

We report observations of 31 compact radio sources using the "Goldstack" interferometer, consisting of the 64-m telescope at Goldstone, California (NASA Deep Space Network) and the 37-m telescope at Tyngsboro, Massachusetts (Haystack Observatory). The baseline is 3900 km (nearly east-west), and the frequency is 7840 MHz, giving a resolution $\lambda/3d = 7 \times 10^{-4}$ sec of arc.

The observing list was mainly organized by selecting sources which had shown compact structure at longer wavelengths (Kellermann *et al.* 1971). The Goldstack interferometer, however, is more versatile than previous intercontinental interferometers with the same resolution. The relatively short Goldstack baseline permits a great range of hour angles to be observed. This, combined with the high sensitivity, allows source structure to be studied in detail.

II. PROCEDURE

The observations were made in two 24-hour periods, on 1971 February 17/18 and 1971 February 28. Right circular polarization was used. Both telescopes were equipped with traveling-wave maser amplifiers. System temperature T_s at Goldstone ranged from about 30° K near the zenith to 40° K near the horizon, but was substantially higher when a strong source such as 3C 84 or 3C 273 was being observed. At Haystack T_s varied from about 50° K near the zenith to 60° K near the horizon. Intermittent rain

* Supported by ONR contract N 00014-67-A00094-0019, NSF grants GP 25225 and GP 19400, and NASA grant 69835.

† Operated by Associated Universities, Inc., under contract with the National Science Foundation.

‡ Supported by NSF grant GP 15436. The Arecibo Observatory is operated by Cornell University under contract to the NSF and with partial support from ARPA.

NOTE.—The NASA/JPL Deep Space Network is operated by the Jet Propulsion Laboratory, California Institute of Technology, under contract NAS7-100 sponsored by the National Aeronautics and Space Administration. Radio astronomy programs at the Haystack Observatory are conducted with support from the NSF.

and snow at Haystack raised T_s to over 100° K for limited periods of time. This also introduced rather large errors since the absorption in the water layer on the Haystack radome could be as high as 20 percent and was not determined accurately.

The NRAO-Cornell Mark I VLB recording system (Bare *et al.* 1967) was used at Goldstone, and at Haystack a compatible recording system which includes a CDC 3300 computer was used. The bandwidth was 330 kHz. Hydrogen-maser frequency standards were used at both antennas to control the digital sampling rates and the local oscillator signals. Processing was done with the Caltech 360/75 computer, using programs written by B. Clark (Clark *et al.* 1968) and by A. Whitney.

The observing procedure consisted of checking the antenna pointing when possible, measuring T_s when on the source, and making two data recordings 8 minutes of time apart. Each data recording is a pair of tapes (one from each end) containing 3 minutes of data.

As with all such VLB experiments, the flux scale is empirically adjusted by an overall scaling factor. Our calibration was accomplished by assuming that four sources—PKS 0106+01, OJ 287, OK 290, and OR 103—were unresolved. The assumption is based on (i) the observation that their fringe amplitudes have a common ratio to their flux densities, (ii) the high cutoff frequency in the spectrum of all four sources (assumed due to synchrotron self-absorption), and (iii) the absence of any variation with hour angle for OJ 287 and OK 290. Any error in scaling is systematic and affects all fringe amplitudes by the same factor. We expect that this error is not greater than ± 10 percent.

Random errors can come from any of the following sources:

1. System noise. In most cases this gives an error of ± 0.05 f.u. For strong sources or in bad weather T_s is increased and the error goes up to ± 0.07 f.u.

2. Antenna pointing and T_s determination. These components generally cause errors of no more than ± 5 percent in fringe amplitude. However, during bad weather the corrections for T_s and for radome transparency become large, and 20 percent of the excess correction is included in the error for fringe amplitude.

3. Cross-correlation coefficient. This coefficient is found by interpolation on a grid of values calculated for a series of time delays and fringe rates. Comparison of results obtained from using the two different computer programs shows that interpolation errors are no more than ± 1 percent. The 3C 273 data also show that calibration differences in the two data sets (February 17/18 and 28) are no more than 5 percent.

4. Phase drifts. In most cases hydrogen-maser oscillators were used at both stations and phase jitter or phase wander was negligible in a 3-minute recording. In a few cases we substituted a Tracor 2.5C crystal oscillator (phase-locked to a rubidium standard) for the maser at Haystack, for test purposes. This gave a phase record which was comparable to the maser for short time scales (< 10 s) but which wandered up to 60° on time scales of 1 min. (The phase-locking loop has a time constant of 40 s.) As a result the error is slightly higher than it would have been with the maser. Comparable phase errors occurred when either antenna was at a very low elevation angle; presumably, this was due to the long atmospheric path.

The errors in Table 1 and Figures 1 and 2 are our estimate of the rms errors from these causes.

III. RESULTS

The results of the observations are given in Table 1. Column (1) gives the source name, and column (2) the date when it was observed (I = February 17/18, II = February 28). Columns (3) and (4) give the identification of the source and its redshift, where known. Columns (5) and (6) contain the E-W (u) and N-S (v) components of the baseline, at the time of observation, in millions of wavelengths. Column (7) gives the total flux of the source and its error. Most of these fluxes were measured at Haystack just prior to the observations. A few others, in parentheses, were measured at 8085 MHz with the NRAO interferometer and corrected to 7840 MHz by using the known spectral

TABLE 1

RESULTS OF THE INTERFEROMETER OBSERVATIONS

Source (1)	Date (2)	Ident. (3)	z (4)	u* (5)	v* (6)	Total Flux (f.u.) (7)	Correlated Flux (f.u.) (8)
PKS 0106+01	II	QSS	2.107	51	+18	2.92±0.05	2.92±0.20
NGC 1052	I	E3	0.0047	70	+ 5	2.74 0.04	0.32 0.06
3C 84	I, II	Seyfert	0.017	†	†	22.5 0.5	†
NRAO 140	I	QSS	1.258	100	+22	2.85 0.15	1.09 0.09
				47	+61		2.19 0.15
CTA 26	II	QSS	0.852	96	+15	3.40 0.07	1.92 0.16
NRAO 150	I			49	+79	8.57 0.16	6.08 0.33
3C 111	II			100	+16	(5.5)	0.62 0.06
3C 120	II	Seyfert	0.033	†	†	9.20 0.20	†
NRAO 190	I			93	+16	1.90 0.05	0.82 0.08
				56	+16		1.40 0.10
OJ 287	II	QSS?		71	− 9	4.10 0.08	4.19 0.22
				85	− 2		4.23 0.22
4C 39.25	I	QSS	0.699	81	−25	11.4 0.2	8.99 0.66
OK 290	II	QSS?		82	−10	2.15 0.04	2.05 0.12
				93	− 2		2.14 0.12
PKS 1127−14	II	QSS	1.187	96	+23	5.9 0.1	2.44 0.13
3C 273	I, II	QSS	0.158	†	†	50.6 0.6	†
3C 274	I	E0(M87)	0.0041	†	†	51.4 0.5	†
3C 279	I	QSS	0.538	†	†	13.3 0.15	†
OQ 208	I	Seyfert	0.077	50	+56	2.50 0.07	1.59 0.10
OR 103	II	QSS?		74	+ 3	3.00 0.06	3.02 0.16
PKS 1508−05	II	QSS	0.361	100	+17	(1.8)	0.78 0.09
DW 1555+00	I	Gal?		71	+16	2.24 0.05	1.78 0.11
DA 406	I	QSS	1.401	58	+60	2.01 0.06	0.68 0.06
NRAO 512	I	QSS		99	+23	(0.8)	0.69 0.06
3C 345	II	QSS	0.595	†	†	11.4 0.15	†
NRAO 530	II	Gal?		86	+27	4.20 0.06	2.50 0.25
3C 371	I	N	0.050	81	+62	1.80 0.07	0.50 0.06
PKS 2134+004	II	QSS	1.936	†	†	13.2 0.2	†
PKS 2145+06	I	QSS	0.367	51	+26	4.44 0.10	3.56 0.19
VRO 42.22.01	I	QSS?		†	†	9.73 0.11	†
3C 466	I	QSS	1.403	97	+19	5.44 0.11	3.08 0.16
3C 454.3	II	QSS	0.859	†	†	11.2 0.2	†
PKS 2345−16	II	QSS	0.6	70	− 5	3.82 0.08	3.03 0.25

* Millions of wavelengths.

† These sources are discussed in the text.

index. Column (8) gives the correlated flux and its error. Daggers in columns (5), (6), and (8) indicate those sources which were observed in detail and are described below.

Table 1 contains six sources not previously detected in long-baseline observations. These include the three Ohio sources (OJ 287, OK 290, and OR 103) used to calibrate the observations, NGC 1052, 3C 111, and 3C 371. 3C 111 is a complex triple source greater than 3′ in extent (Mackay 1969), and is discussed by Broderick *et al.* (1972).

NGC 1052 is an E3 galaxy containing a radio core known to be less than 2″ in diameter (Heeschen 1968). Table 1 shows that the core contains nearly half the flux at 3.8 cm, and that its size is less than ~0″.001. It is comparable with the small component in M87 in both angular size and distance, and therefore is also no more than a few light-months across (see below). M87, however, contains a very much stronger halo than NGC 1052.

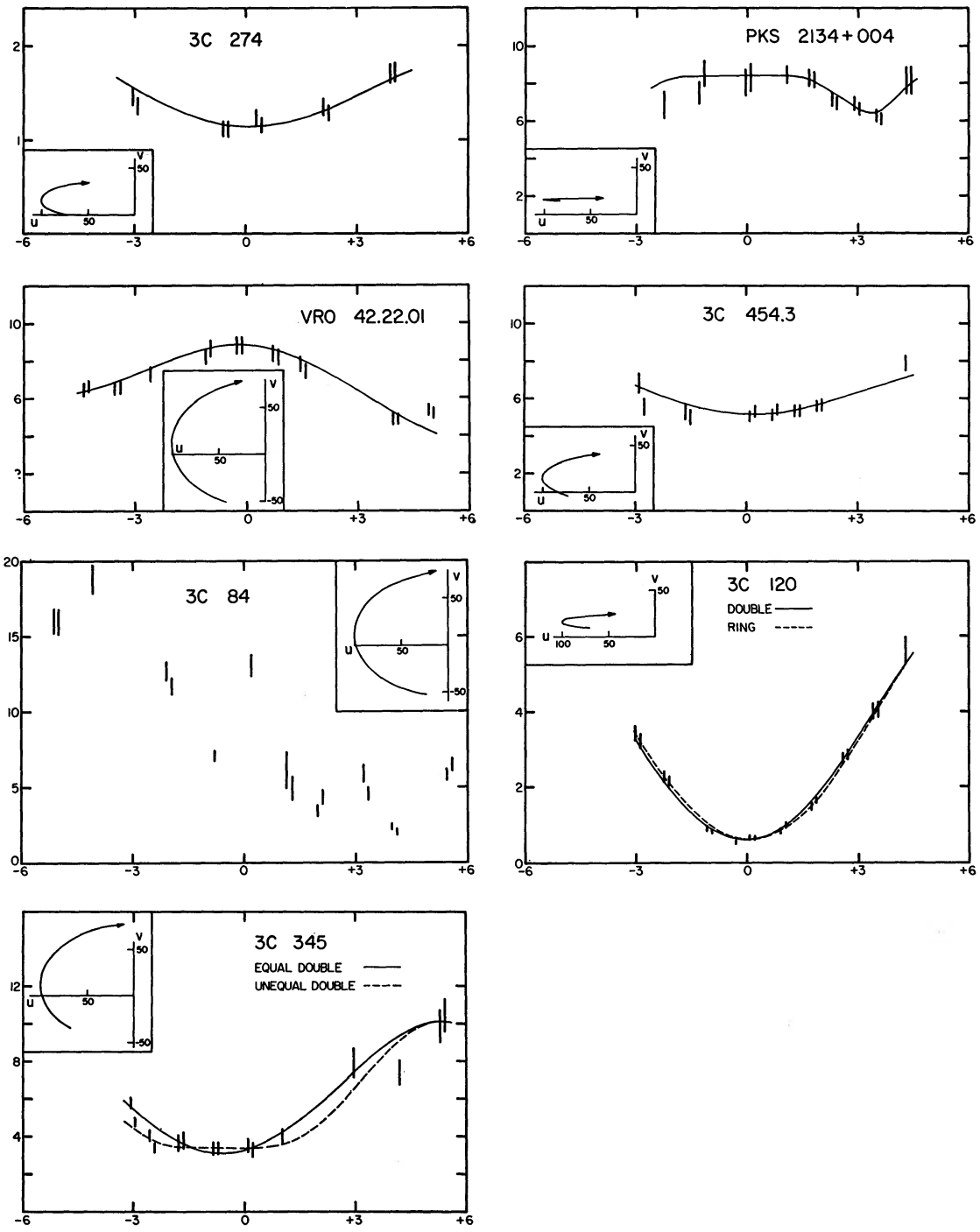

FIG. 1.—Fringe-amplitude data for the Goldstone-Haystack interferometer. Vertical scales are correlated flux density (in flux units), horizontal scales are hour angle from the interferometer meridian (in hours). Insets show the (u, v)-plane coverage for each source. Inset scales are in millions of wavelengths.

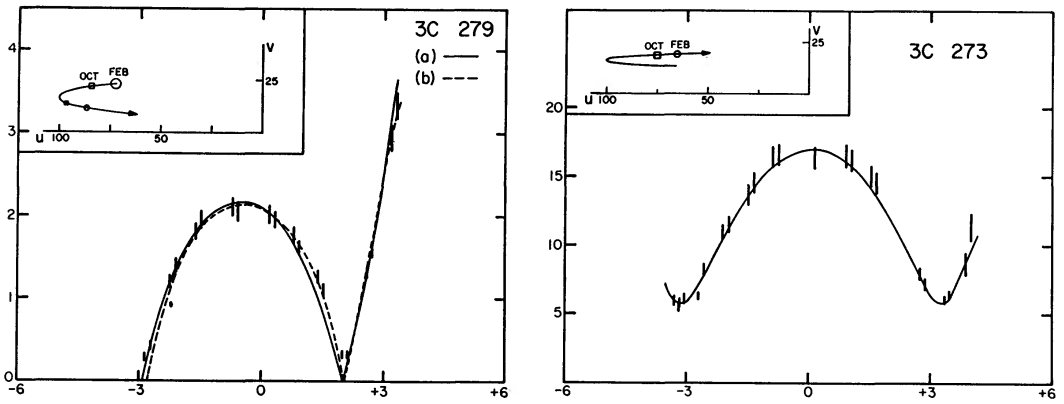

FIG. 2.—Data for the two expanding sources. Scales are the same as Fig. 1. Squares and circles on the u-v tracks indicate the locations of the visibility minima in 1970 October and 1971 February, respectively.

IV. SOURCE STRUCTURE

Nine sources were looked at in sufficient detail that curves of visibility versus hour angle could be drawn. These are divided into two groups: weakly resolved sources and strongly resolved sources. The four weakly resolved sources (3C 274, PKS 2134+004, VRO 42.22.01, 3C 454.3) show a small hour-angle effect, and the visibility does not drop below 0.5 (for the compact component). A great variety of models, of course, could fit the data in each case, and only the simplest models were tried. In two cases, 3C 274 and 3C 454.3, a circular disk fitted reasonably well, and no attempt was made to fit a more complicated model.

The strongly resolved sources (3C 84, 3C 120, 3C 273, 3C 279, 3C 345) were observed close to or beyond a minimum in the visibility function, and this restricted the possible range of models. For each of these sources several simple models were tried, including circular and elliptical disks and rings, and various doubles. One or two models which fit the data are shown for each source. It should be emphasized that these are the simplest models which fit the data and that the true structures are probably more complex. Measurements at many more baselines are required before the true shapes can be found.

a) Weakly Resolved Sources

Figure 1 shows the fringe amplitude (in flux units) versus hour angle from the interferometer meridian (IHA). Also shown is the Fourier-transform plane (the [u, v]-plane) containing the track of the observations. Hour angle increases in the direction of the arrow. The interferometer has maximum resolution near IHA = 0^h, at the vertex of the track.

i) *3C 274 (M87)*

The data for 3C 274 show a significant systematic variation of visibility with hour angle. The line in Figure 1 shows the expected curve for a uniform circular disk of diameter $0''.0013$ and strength 2.0 f.u. The total flux density of 3C 274 is 51.4 f.u.; most of this comes from the larger components which are totally resolved at these spacings.

At 13 cm the compact radio component lies within $1''$ of the optical nucleus of M87, and there is no similar component along the jet (Cohen *et al.* 1969). The present observations at 3.8 cm also show no compact component along the jet, to a level of about 0.4 f.u. The angle $0''.0013$ corresponds to a linear size of 3.8 light-months at 14.8 Mpc, the distance to M87 (Sandage 1968).

Graham (1971) has shown that M87 has a compact component having flux variations at $\lambda = 6$ cm. However the interferometer observations at 3.8 and 13 cm do not give

evidence for expansion or for the existence of several components. A compact component with diameter less than 0".05 was seen at 11 cm in 1966 by Palmer *et al.* (1967). If this is the same object we see at 3.8 cm, the expansion velocity is small, $\leq 0.04\ c$.

ii) *PKS 2134+004*

This source is nearly on the equator, and the u-v track has degenerated to a line. This means that the visibility should be symmetric about IHA = 0. Our data show this consistency, although the points for IHA < 0 have rather large errors since they were taken during bad weather.

The source cannot be an equal double because the minimum visibility is not zero. The simplest model consistent with the data is an unequal point double with separation 0".017, position angle P.A. = −9°.5, and containing 8.4 f.u. (64 percent of the total flux). The ratio between the intensities of the two components (the "component ratio") is 7.5. The expected curve for this model is shown in Figure 1. Unequal double models with position angles near 90° are also possible, but require finite sizes for the components. A "point" component is one which has diameter less than about 0".0005.

iii) *VRO 42.22.01 (BL Lac)*

Circularly symmetric models are ruled out since the fringe visibility γ varies strongly with position angle; at IHA = $-2^h.5$ and $+4^h$ the baseline is $85 \times 10^6\ \lambda$ in position angles 110° and 35°, but $\gamma = 0.75$ and 0.51, respectively. It is not clear whether we have observed a minimum near IHA = $+4^h.5$ since the last two points were made at a large zenith angle and are less reliable than the others. The curve in Figure 1 fits all but the last two points, and comes from the simplest model, an equal point double with separation 0".0009, P.A. = 174°, and containing 8.8 f.u. (90 percent of the total). Unequal point double models as well as elliptical disks give comparable fits to the observed data.

iv) *3C 454.3*

The endpoints indicate that the source is partially resolved, and is not a "point" with strength 5–6 f.u. The curve is for a uniform circular disk 0".0012 in diameter, with strength 8.3 f.u. (74 percent of the total). The fit is only fair, and suggests that the structure may be more complex. It could, for example, be a "core-halo" with an unresolved component of strength 5 f.u. and another with a diameter greater than ~0".002. Various doubles would also fit the data. The spectrum and interferometric observations at longer wavelengths with comparable resolution (Kellermann *et al.* 1971) suggest the existence of several components with different sizes and spectra.

b) Strongly Resolved Sources

i) *3C 84 (NGC 1275)*

This source is distinguished from the others by the complex behavior of its visibility function, which appears to have six extrema along the observed locus. This suggests the presence of several discrete components with sizes less than ~0".001 and separations in the neighborhood of 0".01. However, much of the scatter may be due to unknown large errors of measurement since there was poor weather during the time these data were obtained.

Previous measurements have shown that 3C 84 is complicated, both in its spatial structure and in the spectra of the various components. The present data presumably refer to the compact core which, at 6 cm, has been interpreted as an expanding disk whose diameter in 1971.2 would have been 0".004 if the expansion were constant (Kellermann *et al.* 1971).

ii) *3C 120*

Two possible models are shown for 3C 120: (*a*) a uniform circular ring of diameter 0".00144 and strength 7.4 f.u. (80 percent of the total) and (*b*) an equal point double of

separation 0".00098, P.A. = 95°, and total strength 6.5 f.u. (71 percent). These fit the data equally well.

A uniform circular disk of diameter 0".00227 fits the data almost as well as the ring. However, it requires 8.5 f.u. (more than 90 percent of the total flux of the source), and this seems somewhat unlikely in view of the complex spectrum. More observations at either longer or shorter baselines could sort out these three possibilities. The fact that γ is small at the minimum suggests that the source has good symmetry. If it is a double, the two components must be equal to within 18 percent or less.

iii) *3C 345*

Circularly symmetric models are ruled out since γ is a function of position angle. The simplest model that fits the data is an equal point double with separation 0".00086 in position angle 103°, containing 88 percent of the flux. The data point at IHA = $+4^h.2$ does not fit this model or any other simple one and, if real, indicates more complex structure.

Two other simple models that reasonably represent the data are (1) an unequal point double with separation 0".0011, P.A. 103°, and containing 85 percent of the flux with a component ratio of 2; and (2) an elliptical disk containing all the flux with axes 0".00045 and 0".00095, and P.A. 103°. The ambiguities arise because it is not clear whether or not our observations include the first minimum of the visibility function. Figure 1 shows the expected curves for the two doubles.

V. EXPANDING SOURCES

We obtained visibility curves for two sources, 3C 273 and 3C 279, for which similar data had been obtained by Knight *et al.* (1971) in October 1970. Our data, taken in February 1971, as well as similar data taken by the MIT-Goddard group, show clear differences from the October data, in the sense that the brightness distribution of both sources has expanded (Jauncey 1971; Shapiro 1971; Whitney *et al.* 1971). The Goldstack interferometer, at the identical wavelength, was used for all these observations.

a) 3C 279 (Figure 2)

Simple equal double models fit the data remarkably well. Figure 2 shows the expected curves for two possibilities, (*a*) separation 0".0016, P.A. 39°, component diameters 0".0008, strength 12.2 f.u. (91 percent of the total); and (*b*) separation 0".0045, P.A. 45°, diameters 0".0008, strength 4.4 f.u. (33 percent of the total). Several other models were also tried. A uniform elliptical disk which fits the data moderately well can be found, but it requires more flux than exists. An elliptical ring does not exceed the flux limit, but does not fit the data as well as the doubles.

The two models shown in Figure 2 show that our data alone do not allow an unambiguous determination of separation. The wider separation fits the data slightly better but appears less likely when previous observations at 13 cm (Moffet *et al.* 1971; Broderick *et al.* 1972) and 3.8 cm (Knight *et al.* 1971) are considered.

The visibility curve for 3C 279 has two striking characteristics, which are discussed later.

1. The nulls are very deep. For model *a*, the minimum fringe visibility $\gamma_m \leq 0.025$; for model *b*, $\gamma_m \leq 0.068$. This means that the two components are equal to 5 percent or less (model *a*) or 14 percent or less (model *b*).

2. The brightness distribution had a notable change in 4 months. Figure 2 shows 5 hours between the nulls (actually two crossings of the same null line). In 1970 October Knight *et al.* (1971), using the identical interferometer, had about $3\frac{1}{2}$ hours between the nulls.

b) 3C 273 (Figure 2)

Most of our observations were evidently beyond the first minimum in the (u, v)-plane, and it is difficult to determine the overall structure without measurements at shorter baselines. If the source is a double, the two components cannot be equal, since then the minima would be zero. No unequal point double gives a good fit, but a fair fit is shown in Figure 2 with a point double of separation 0".00155, P.A. 60°, and intensities of 15.9 and 10.2 f.u. (52 percent of the total flux). The measured points show a systematic departure from this model, being flatter near IHA = 0^h and possibly rising more sharply at IHA = $+4^h$, suggesting complex extended structure. The uncertainty of this model is great emough that the axis could be aligned with the optical "jet" at P.A. 43°.

A uniform circular ring of diameter 0".0023 and strength 42.8 f.u. (82 percent of the total) fits the data better than the double near IHA = 0. However, its visibility goes to zero, whereas the residual flux at the minima is 6 f.u., or 12 percent of the total. A uniform disk gives a worse fit, requiring more flux than exists. If the source is basically circular in shape, it must be nonuniform with strong limb brightening.

3C 273 has a complex spectrum. Observations at 18 and 6 cm have suggested four components (Kellermann *et al.* 1971). Two components have sizes 0".002 or smaller and approximately equal strength at 3.8 cm; these may form most of the source we observe with the Goldstack interferometer.

Comparison of the October 1970 data of Knight *et al.* (1971) with our data shows a significant change in the visibility function. The two minima are not clearly defined, as they are for 3C 279, but a change in their separation is apparent. In 1971 February the separation was about 7 hours whereas in 1970 October the separation was perhaps 5 hours. Moreover, the ratio of maximum to minimum fringe visibility almost doubled in 4 months. This change may also be explained by a simple expansion: the minimum flux is constant, but in February the separation was larger and the observations went farther up the second maximum of the visibility function.

c) Expansion Rates

The *u-v* tracks for 3C 279 and 3C 273 are shown in Figure 2. The observed minima from 1971 February are shown as circles on the tracks, with the size of the circle indicating the error in finding the hour angle of the minimum. Squares indicate the minima in 1970 October, as reported by Knight *et al.* (1971).

An angular expansion rate which is nearly model-independent can be calculated in the following way. Assume that the expansion is conformal (only the scale of the visibility function changes with time). The corresponding October and February minima are nearly on the same radius vector, so the relative change in radius approximately gives the expansion rate. Table 2 shows the radii to the measured minima in reciprocals of the wavenumber, i.e., in radians, and the yearly rate $s(R_{\text{Feb}} - R_{\text{Oct}})$, where s scales the observations to 1 year. This rate is a measure of the true angular expansion. The two entries in Table 2 for 3C 279 correspond to the minima measured near (1) rising and (2) setting.

TABLE 2

EXPANSION OF 3C 273 AND 3C 279

Source	R_{Oct} (rad)	R_{Feb} (rad)	Rate (rad yr^{-1})
3C 273.....	$1.28 \pm .02 \times 10^{-8}$	$1.45 \pm .03 \times 10^{-8}$	4.8×10^{-9}
3C 279(1)....	$1.16 \pm .02 \times 10^{-8}$	$1.28 \pm .04 \times 10^{-8}$	3.5×10^{-9}
3C 279(2)....	$1.04 \pm .01 \times 10^{-8}$	$1.15 \pm .02 \times 10^{-8}$	3.2×10^{-9}

The conversion of the values in Table 2 to true angular or linear rates is model-dependent. For example, a uniform ring has an angular-diameter expansion rate given by 0.765 times the rate in Table 2. A double has an angular-separation expansion rate given by 0.500 cos (Φ − P.A.) times the rate in Table 2, where P.A. is the position angle of the axis of the double and Φ the position angle of the observations.

We calculate a linear expansion rate by assuming that each source is a double (the close double for 3C 279) and that its redshift is the normal measure of distance. The observed angular separation is

$$\Theta_0 = y/D ,$$

where the metric distance D is

$$D = \frac{c}{H_0 q_0^2 (1 + z)} \{q_0 z + (q_0 - 1)[(1 + 2q_0 z)^{1/2} - 1]\}$$

(Sandage 1961, 1965). The linear rate of each component (at the source) is

$$\frac{1}{2}\frac{dy}{dt_1} = \tfrac{1}{2}(1 + z)\frac{dy}{dt_0} = \tfrac{1}{2}(1 + z) D \frac{d\Theta_0}{dt_0}$$

where $d\Theta_0/dt_0$ is the observed angular rate. Table 3 shows the results, for $H = 75$ km s^{-1} Mpc^{-1} and $q_0 = +1$. The last column gives the apparent transverse velocity, normalized by the velocity of light.

VI. DISCUSSION

The apparent velocities in Table 3 are greater than the speed of light. We shall call this "super-light expansion." Gubbay *et al.* (1969) and Moffet *et al.* (1971) first showed super-light expansion in 3C 279 at 13 cm, by comparing variations measured with a trans-Pacific interferometer with variations in total flux. They deduced $v/c \gtrsim 2$. Our observations (Jauncey 1971) and those of the MIT-Goddard group (Shapiro 1971; Whitney *et al.* 1971) confirm this result as well as the super-light expansion for 3C 273 and 3C 279 reported by Knight *et al.* (1971). A slower expansion has been reported by Kellermann *et al.* (1971) for the Seyfert galaxy 3C 84, who give $v/c \approx \frac{1}{3}$ at $\lambda = 6$ cm, based on trans-Atlantic measurements in 1968 and 1969.

The possibility of super-light expansion was suggested by Rees (1967) as a way to reduce the excessive energy requirements of synchrotron models for rapidly varying radio sources. A relativistically moving object with Lorentz factor $\gamma = (1 - v^2/c^2)^{-1/2}$ can display an apparent transverse velocity of up to γv. The maximum is attained for motion directed at an angle $\sin^{-1}(1/\gamma)$ to the line of sight, and the corresponding Doppler shift is γ. If the variable source is a symmetric expanding double in the rest frame of 3C 279, the axis of expansion must be oriented so that one component is blueshifted by $\gtrsim 3$ and the other is redshifted by $\gtrsim 3$. However, this model meets severe difficulties when faced with the requirement, for 3C 279, that the two components of the "double"

TABLE 3

EXPANSION RATES*

Source	z	D (Mpc)	Φ−P.A.	$d\Theta_0/dt_0$ (rad yr^{-1})	v/c
3C 273....	0.158	470	13°.5	2.3×10^{-9}	2
3C 279....	0.538	910	40°	1.3×10^{-9}	3

* Deceleration parameter $q_0 = +1$ and $H = 75$ km s^{-1} Mpc^{-1} are assumed.

must be nearly equal. If the two components are intrinsically identical with flux $S_\nu \propto \nu^\alpha$, the ratio of the observed flux densities would be $\{[1 + (v/c)\cos\theta]/[1 - (v/c)\cos\theta]\}^{3-\alpha} \approx (20)^{3-\alpha}$, where θ is the angle between the expansion axis and the line of sight (Ryle and Longair 1967). The observed equality can be obtained only by having the components evolve in an artificial way. (This general problem has been discussed by Ozernoy and Sazonov 1969). Furthermore, as B. G. Clark has pointed out, in 1968 the total flux from 3C 279 was not great enough for this possibility. The required evolution is very rapid, and the approaching component in 1968 would have to have had a flux on the order of 100 f.u. at a wavelength of a few millimeters, which did not exist.

A variation of this model (suggested by Rees) is that we may be seeing two approaching components out of many that were shot out during an explosion. They have the appropriate blueshift and swamp the flux from components moving in other directions. This situation is similar to Woltjer's model (1966), which envisages a relativistic outflow of particles along radial field lines. The required symmetry of the "double" is still a problem, however. For this reason we investigated expanding elliptical disks and rings, but, as described above, we were unable to fit the data satisfactorily.

There are other possible explanations for the super-light expansions. The apparent motion may be a "searchlight" effect: the excitation of existing material by a shock front from a central object. The super-light expansion associated with Nova Persei was satisfactorily explained this way (Couderc 1939). Many variations of this mechanism are possible.

It is also possible that there are no motions at all, merely properly phased time variations in a stationary ensemble of sources. In particular, if in a stationary triple source the ratio of flux densities of the outer components to the inner component increases with time, then the source will appear to expand. In the case of 3C 279, however, the total flux density at 3.8 cm remained constant between 1970 October and 1971 February (Dent and Kajoian, private communication). Thus, this model appears as artificial as relativistic expansion.

Another way to explain the observed equality of the components is if they are simply two images of the same source, such as might be produced by gravitational focusing around a foreground star (Barnothy and Barnothy 1969). The expansion is due to relative motion of the star and the Earth. This model predicts that approximately equal numbers of sources should be expanding and contracting, although the two we have observed are both expanding.

Finally, we remark that the entire super-light problem disappears if we drop the assumption that the redshift is the usual measure of distance, and instead assume that both 3C 273 and 3C 279 are closer than 100 Mpc.

VII. SUMMARY

The data obtained from our limited coverage of the (u, v)-plane have disclosed complex structure in the compact components of radio galaxies and QSSs. Such structure seems similar to that observed at larger scale. It is remarkable that radio sources having a range of more than 10^5 in angular size exhibit this similarity.

Two QSSs have data from an earlier epoch, 3C 273 and 3C 279 (Knight *et al.* 1971). They both show super-light expansion. The Seyfert galaxy NGC 1275 (3C 84) has an angular expansion rate comparable to that observed for 3C 273 and 3C 279, but the apparent linear rate is less than c (Kellermann *et al.* 1971). The physically smallest radio object, in the nucleus of M87, does not appear to show any expansion, and a limit of 0.04 c is suggested. These results may indicate that in galaxies the expansion rate is diminished by the effect of the interstellar medium, or that the super-light rate observed for QSSs is an artifact of the assumption that their large redshift is a measure of distance.

The measurements of total flux density at 3.8 cm were made at Haystack by Drs. W. Dent and G. Kajoian, and we are grateful to them for giving us these data. We thank Dr. I. Shapiro for discussing with us the results of the 1970 October observations before their publication. We are grateful to Drs. M. Rees, B. Clark, and R. Ekers for several illuminating discussions, and to A. Whitney, who spent several days helping us organize his computer program at Caltech. We thank D. Spitzmesser and L. Skjerve of JPL for their assistance at Goldstone, and A. E. E. Rogers for his assistance at Haystack. We thank the referee for helpful comments. D. B. S. is an NSF Graduate Fellow.

REFERENCES

Bare, C., Clark, B. G., Kellermann, K. I., Cohen, M. H., and Jauncey, D. L. 1967, *Science*, **157**, 189.
Barnothy, J. M., and Barnothy, M. F. 1969, *Bull. A.A.S.*, **1**, 181.
Broderick, J. J., Kellermann, K. I., Shaffer, D. B., and Jauncey, D. L. 1972, submitted to *Ap. J.*
Clark, B. G., Kellermann, K. I., Bare, C. C., Cohen, M. H., and Jauncey, D. L. 1968, *Ap. J.*, **153**, 705.
Cohen, M. H., Moffet, A. T., Shaffer, D., Clark, B. G., Kellermann, K. I., Jauncey, D. L., and Gulkis, S. 1969, *Ap. J.* (*Letters*), **158**, L83.
Couderc, P. 1939, *Ann. d'ap.*, **2**, 271.
Graham, I. 1971, *Nature*, **231**, 253.
Gubbay, J., Legg, A. J., Robertson, D. S., Moffet, A. T., Ekers, R. D., and Seidel, B. 1969, *Nature*, **224**, 1094.
Heeschen, D. S. 1968, *Ap. J.* (*Letters*), **151**, L135.
Jauncey, D. L. 1971, paper presented at Rumford Symposium, American Academy of Arts and Sciences.
Kellermann, K. I., Jauncey, D. L., Cohen, M. H., Shaffer, D. B., Clark, B. G., Broderick, J., Rönnäng, B., Rydbeck, O. E. H., Matveyenko, L., Moiseyev, I., Vitkevitch, V. V., Cooper, B. F. C., and Batchelor, R. 1971, *Ap. J.*, **169**, 1.
Knight, C. A., Robertson, D. S., Rogers, A. E. E., Shapiro, I. I., Whitney, A. R., Clark, T. A., Goldstein, R. M., Marandino, G. E., and Vandenberg, N. R. 1971, *Science*, **173**, 52.
Mackay, C. D. 1969, *M.N.R.A.S.*, **145**, 31.
Moffet, A. T., Gubbay, J., Robertson, D. S., and Legg, A. J. 1971, *Proc. I.A.U. Symp. No. 44* (in press).
Ozernoy, L. M., and Sazonov, V. N. 1969, *Ap. and Space Sci.*, **3**, 395.
Palmer, H. P., Rowson, B., Anderson, B., Donaldson, W., Miley, G. K., Gent, H., Adgie, R. L., Slee, O. B., and Crowther, J. H. 1967, *Nature*, **213**, 789.
Rees, M. J. 1967, *M.N.R.A.S.*, **135**, 345.
Ryle, M., and Longair, M. S. 1967, *M.N.R.A.S.*, **136**, 123.
Sandage, A. R. 1961, *Ap. J.*, **133**, 355.
———. 1965, *ibid.*, **141**, 1560.
———. 1968, *Ap. J.* (*Letters*), **152**, L149.
Shapiro, I. I. 1971, paper presented at Rumford Symposium, American Academy of Arts and Sciences.
Whitney, A. R., Shapiro, I. I., Rogers, A. E. E., Robertson, D. S., Knight, C. A., Clark, T. A., Goldstein, R. M., Marandino, G. E., and Vandenberg, N. R. 1971, *Science*, **173**, 225.
Woltjer, L. 1966, *Ap. J.*, **146**, 597.